


RESEARCH PAPER



Identification of guanine nucleotide exchange factors that increase Cdc42 activity in primary human endothelial cells

Nathalie R. Reinhard^a, Sanne Van Der Niet^a, Anna Chertkova^a, Marten Postma^a, Peter L. Hordijk^{a,b}, Theodorus W. J. Gadella Jr.^a, and Joachim Goedhart ^a

^aMolecular Cytology, Swammerdam Institute for Life Sciences, van Leeuwenhoek Centre for Advanced Microscopy, University of Amsterdam, Amsterdam, The Netherlands; ^bDepartment of Physiology, Amsterdam University Medical Center, location VUmc, Amsterdam, The Netherlands

ABSTRACT

The Rho GTPase family is involved in actin dynamics and regulates the barrier function of the endothelium. One of the main barrier-promoting Rho GTPases is Cdc42, also known as cell division control protein 42 homolog. Currently, regulation of Cdc42-based signalling networks in endothelial cells (ECs) lack molecular details. To examine these, we focused on a subset of 15 Rho guanine nucleotide exchange factors (GEFs), which are expressed in the endothelium. By performing single cell FRET measurements with Rho GTPase biosensors in primary human ECs, we monitored GEF efficiency towards Cdc42 and Rac1. A new, single cell-based analysis was developed and used to enable the quantitative comparison of cellular activities of the overexpressed full-length GEFs. Our data reveal GEF dependent activation of Cdc42, with the most efficient Cdc42 activation induced by PLEKHG2, FGD1, PLEKHG1 and PREX1 and the highest selectivity for FGD1. Additionally, we generated truncated GEF constructs that comprise only the catalytic dbl homology (DH) domain or together with the adjacent pleckstrin homology domain (DHPH). The DH domain by itself did not activate Cdc42, whereas the DHPH domain of ITSN1, ITSN2 and PLEKHG1 showed activity towards Cdc42. Together, our study characterized endothelial GEFs that may directly or indirectly activate Cdc42, which will be of great value for the field of vascular biology.

ARTICLE HISTORY

Received 6 February 2019
Revised 9 July 2019
Accepted 8 August 2019

KEYWORDS

Rho GEF; guanine exchange factor; Cdc42; Rac1; endothelial cells; FRET biosensor; image analysis; fluorescent protein

Introduction

The Rho family of small GTPases belongs to the superfamily of Ras GTPases. Approximately 20 Rho GTPases have been identified, some of which show >85% homology and functional redundancy [1,2]. Via differential actin cytoskeleton remodelling, Rho GTPases regulate a range of cellular responses, including cell adhesion, -migration and -polarity [3]. In the endothelium, these processes form the basis of vascular homeostasis and dynamic regulation of endothelial barrier function. Consequently, Rho GTPases are key molecular components in EC biology.

Rho GTPases act as molecular switches, and their activation and downstream signalling is regulated by three groups of proteins [4]. While Rho guanine nucleotide exchange factors (GEFs) mediate the Rho GTPase GDP-GTP exchange, leading to an activated GTPase, the intrinsic GTP hydrolysis, i.e. inactivation, is stimulated by Rho GTPase activating proteins (GAPs). Additionally, members of the Rho guanine dissociation inhibitors (GDI) family, sequester inactive Rho GTPases in the cytoplasm, securing a large pool of Rho GTPases available

for rapid cellular responses to external cues. Roughly 80 GEFs, 70 GAPs and 3 GDIs have been identified, greatly outnumbering the ~20 Rho GTPases. Consequently, the regulation of Rho GTPase activity, both in time and place, is highly complex [3,4].

GEFs comprise the largest group of Rho GTPase regulators, consisting of two families; 11 dedicator of cytokinesis (Dock) proteins – and 74 diffuse B-cell lymphoma (Dbl) proteins [5–13]. The Dbl family has been repeatedly linked to Rho activation. Members of this family contain a Dbl-homology (DH) domain of around 170–190 residues, that regulates the Rho GTPase GDP-GTP exchange [10,13]. In addition, the majority of DH-containing Dbl-family members encode a pleckstrin homology (PH) domain of approximately 120 residues. PH domains can contribute to GEF autoinhibition, activity regulation, sub-cellular localization, phospholipid binding and to the scaffolding of related signalling proteins [4,10,14]. However, these functions are relatively unexplored and in general PH-domain specific functions are poorly documented.

CONTACT Joachim Goedhart  j.goedhart@uva.nl  Molecular Cytology, Swammerdam Institute for Life Sciences, van Leeuwenhoek Centre for Advanced Microscopy, University of Amsterdam, Amsterdam, The Netherlands

© 2019 The Author(s). Published by Informa UK Limited, trading as Taylor & Francis Group.
This is an Open Access article distributed under the terms of the Creative Commons Attribution-NonCommercial-NoDerivatives License (<http://creativecommons.org/licenses/by-nc-nd/4.0/>), which permits non-commercial re-use, distribution, and reproduction in any medium, provided the original work is properly cited, and is not altered, transformed, or built upon in any way.

Although GEF-Rho GTPase interactions are critical determinants in Rho GTPase signalling networks, molecular details are still missing. Additionally, current studies are mostly based on studies with isolated components or pull-down experiments on lysed cells. The *in vitro* data provide mechanistic details [13], but lack physiological relevance due to the absence of cellular context. Here, we specifically focused on GEF-Cdc42 interactions in the cellular environment, with special emphasis on the endothelium. We selected a subset of endothelial GEFs and performed fluorescence resonance energy transfer (FRET) measurements to measure Cdc42 activation in live primary HUVECs (human umbilical vein endothelial cells). This single-cell FRET-based approach identifies critical activators of Cdc42 in the endothelium.

Results

Cdc42 GEF selection in human ECs

Over the past years, the Rho GTPase Cdc42 has been identified as a key regulator in endothelial barrier control [15–18]. Endothelial barrier function is dependent on tight orchestration of complex, interacting signalling pathways, of which detailed information is still missing. To explore Cdc42-mediated signalling networks in ECs, we here tested a series of potential Cdc42 GEFs for their selectivity and effectivity in activating Cdc42.

Potential Cdc42 GEFs were selected, based on (i) expression level analysis; (ii) catalytic Rho GEF activity (mostly based on *in vitro* studies); and (iii) reported effects on (barrier) function in ECs [13,19–21]. Following these criteria, 15 GEFs were identified to be of interest; these include α -Pix, Asef2, β -Pix, FGD1, FGD5, ITSN1, ITSN2, PLEKHG1, PLEKHG2, PLEKHG4, PREX1, SGEF, TrioN, TUBA and Vav2. Except for TUBA (lacking PH domain), these GEFs all contain a DH and a PH domain, positioning them as members of the Dbl GEF family. A schematic overview of the domain organization within these GEFs was obtained using the SMART (Simple Modular Architecture Research Tool) database [22], and is illustrated in Figure 1.

GEF-phenotypes in ECs

Most of the selected GEFs have not been previously studied in ECs. The initial characterization of their potential function entailed analysis of their intracellular localization. Unfortunately, due to the lack of proper antibodies, it is not possible to study localization of the endogenous proteins. Therefore, we generated GEF fusions with the cyan fluorescent protein mTurquoise2 (mTq2), to explore individual GEF localization.

Analysis of expression of mTq2-GEFs in confluent EC monolayers was combined with immunofluorescent staining for F-actin and the cell-cell contact protein Vascular Endothelial (VE)-cadherin (Figure 2(a)). This strategy induced notable phenotypes in ECs, which are qualitatively described below. A specific ‘protruding’ phenotype was observed for FGD1, PLEKHG2 and Vav2. In cells expressing these GEFs, the peripheral membrane protrudes beyond the VE-cadherin-positive cell-cell junction, a phenomenon that is also induced by the expression of constitutively active Cdc42 (Cdc42-G14V) (Figure 2(b)). FGD1 and Vav2 furthermore show a marked increase in cortical actin, while PLEKHG2 itself partly localized at F-actin fibres.

In contrast to this protruding phenotype, expression of β -Pix resulted in a ‘contractile’ phenotype, marked by an increase in F-actin stress fibres and a jagged appearance of the VE-cadherin complex.

While most of the GEFs showed homogeneous localization throughout the cell, localization to vesicle-like structures was observed for ITSN1, ITSN2 and TUBA. Expression of PLEKHG1 and PREX1, induced a large fraction of cortical actin. Next to this induction of cortical actin, we observed dissociation from the cell matrix, combined with reduced levels of VE-cadherin at cell-cell junctions. TrioN positive cells, showed nuclear accumulation and a typical linear VE-cadherin phenotype. These linear VE-cadherin junctions have already been reported as a TrioN-specific phenomenon [23–25]. No specific phenotypes were observed for α -Pix, Asef2, FGD5 and PLEKHG4.

Together, these data localize mTq2-tagged GEFs in human ECs and show that the GEFs induce specific and differential phenotypes, inferred from endogenous F-actin- and VE-cadherin labelling.

A single-cell FRET-based approach to study GEF activation of Cdc42

The GEF localization approach revealed various GEF-specific phenotypes in ECs. Although some of these phenotypes hint towards the activation of Cdc42, direct evidence is lacking. In order to study GEF-mediated Cdc42 activation directly, we applied a single-cell FRET-biosensor imaging strategy, summarized in Figure 3. This strategy involves a FRET biosensor which records Cdc42 activation [26]. The sensor read-out uses a cyan fluorescent protein (CFP) and a yellow fluorescent protein (YFP) as a FRET pair that allows ratiometric image-based analysis, in which an increase in YFP/CFP ratio corresponds to an increase in Cdc42 activation.

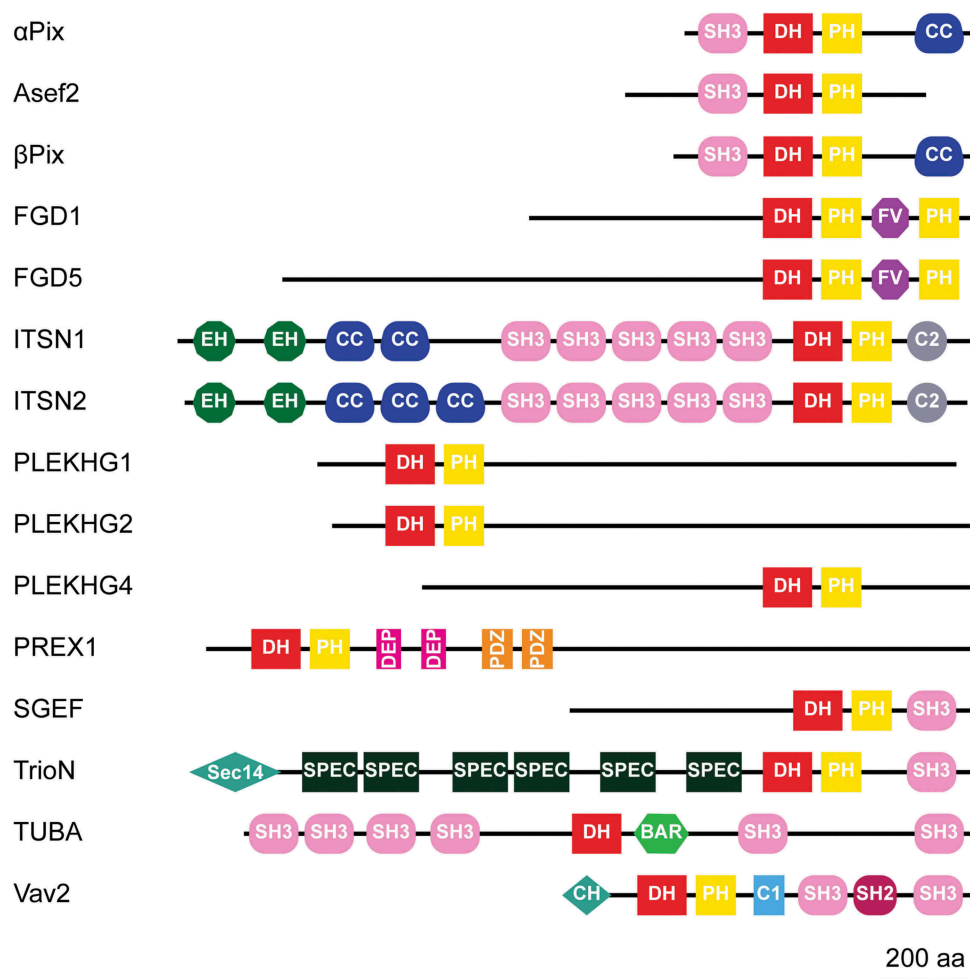


Figure 1. Protein domain structure of potential Cdc42 GEFs.

Size of GEF structure relates to number of amino acids. Scale bar = 200 amino acids (aa). SH3 = Src homology 3; DH = Dbl homology; PH = Pleckstrin homology; CC = coiled coil; FV = FYVE domain; EH = Eps 15 homology; C2 = Protein kinase C conserved region 2; DEP = domain found in Dishevelled, EGL-10 and pleckstrin; PDZ = domain present in PSD-95, Dlg homologous region and ZO-1/2; Sec14 = domain in homologous of a *S. cerevisiae* phosphatidylinositol transfer protein; SPEC = spectrin repeat; BAR = Bin-Amphiphysin-Rvs; CH = Calponin homology domain; C1 = Protein kinase C conserved region 1; and SH2 = Src homology 2.

In our experimental setup, the Cdc42 sensor is co-expressed with either a soluble mCherry (as a control) or a mCherry-tagged GEF of interest. The fluorescence intensity of mCherry will reflect the concentration of the GEF. Cells that showed both sensor as well as mCherry expression within the intensity range of 4–600, were selected. Next, image acquisition and processing resulted in a ratiometric YFP/CFP image, including a corresponding average YFP/CFP value. These average YFP/CFP values of multiple cells were plotted for both the control as well as for the GEF-expressing cells (Figure 3). In turn, YFP/CFP ratios and corresponding mCherry intensities were plotted in mCherry-YFP/CFP ratio graphs (supplementary Figure S1). The rationale is that the Rho GTPase activity, assessed from the YFP/CFP ratio, is correlated

with GEF activity, inferred from mCherry fluorescence. To quantify the relationship between activity and GEF concentration, the data points (each dot represents a single cell) were subjected to linear regression analysis via the Theil–Sen estimator method. The Theil–Sen estimator method calculates the median slope, which we take as a measure of the relative activity of a GEF. For a quantitative comparison between conditions, we plot the median activity and the 95% confidence interval (Figure 3). Details of this Theil–Sen estimator analyses are summarized in Supplemental Figure S1.

In summary, the cell-based analysis of Rho GTPase activation with FRET-based biosensors and tagged GEFs enables the determination and direct quantitative comparison of GEF activity in single living ECs.

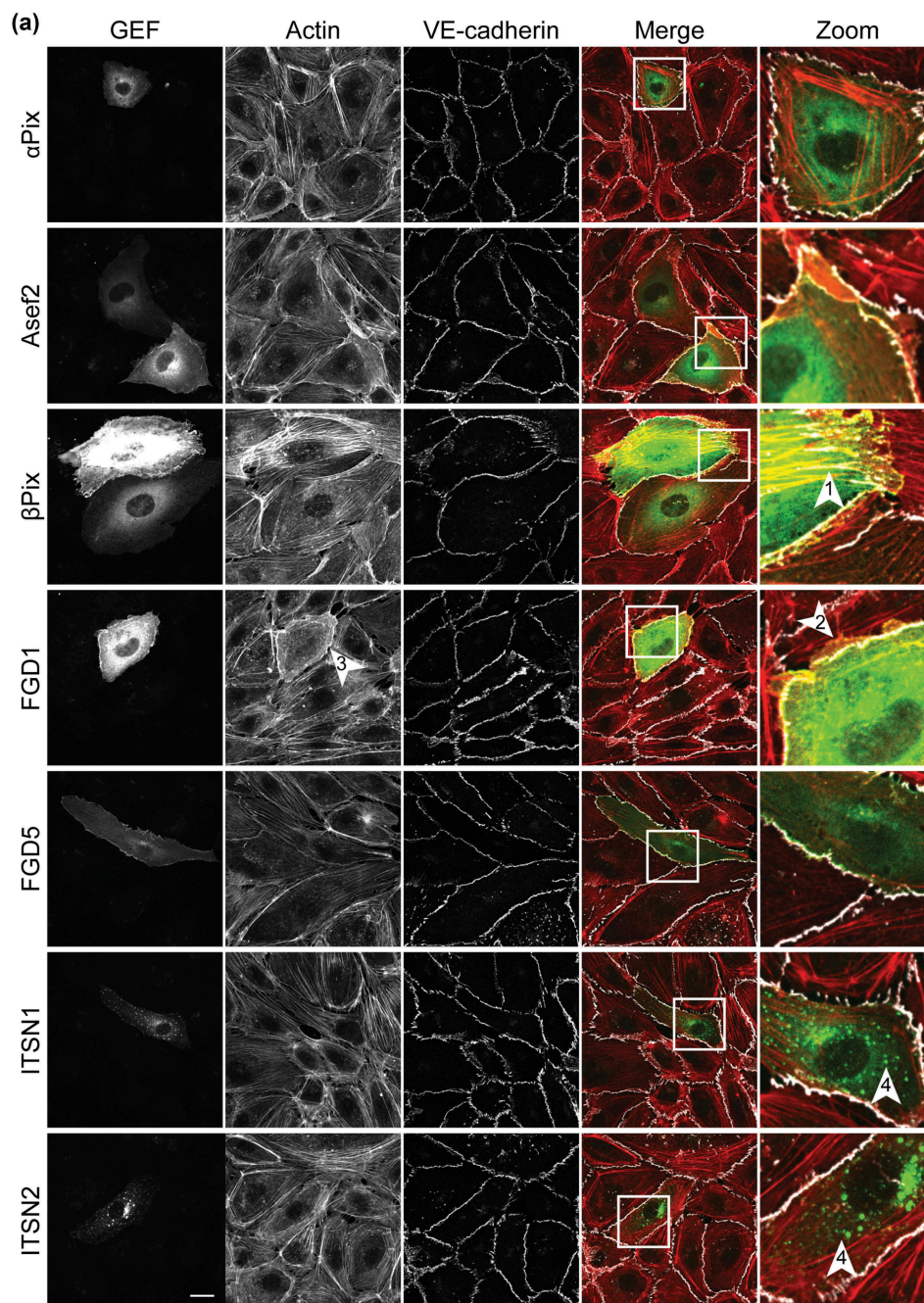


Figure 2a. Ectopic expression of potential Cdc42 GEFs induces specific phenotypes in ECs.

(a) ECs were transiently transfected with mTq2-fused α -Pix, Asef2, β -Pix, FGD1, FGD5, ITSN1, ITSN2, PLEKHG1, PLEKHG2, PLEKHG4, PREX1, TrioN, TUBA or Vav2. ECs were grown to a monolayer and stained for F-actin and VE-cadherin. Arrowheads highlight specific phenotypes: arrowhead #1 contractile phenotype, arrowhead #2 protruding phenotype, arrowhead #3 cortical actin, arrowhead #4 vesicle-like structures, arrowhead #5 linear VE-cadherin. Except for the zoomed images, image acquisition and processing are equal between all conditions. (b) ECs were transiently transfected with Cdc42-G14V, grown to a semi-confluent monolayer and stained for F-actin and VE-cadherin. Arrowhead #2 indicates protruding phenotype, Arrowhead #3 indicates cortical actin. Scale bars of **A** and **B** are 20 μ m.

GEF expression induces specific Cdc42 and Rac1 activation patterns in ECs

The workflow described in the previous section was applied for all selected GEFs listed in Figure 1. First, the YFP over CFP ratios were determined for ectopically expressed GEFs. (Figure 4(a)). Next to Cdc42

activation also Rac1 activation was monitored, using a validated Rac1 FRET sensor[25] (Figure 4(b)). The YFP/CFP ratios were subsequently converted into ‘relative activity’ values by taking GEF expression levels into account. The resulting activities are sorted according to their median value and plotted with a 95% confidence

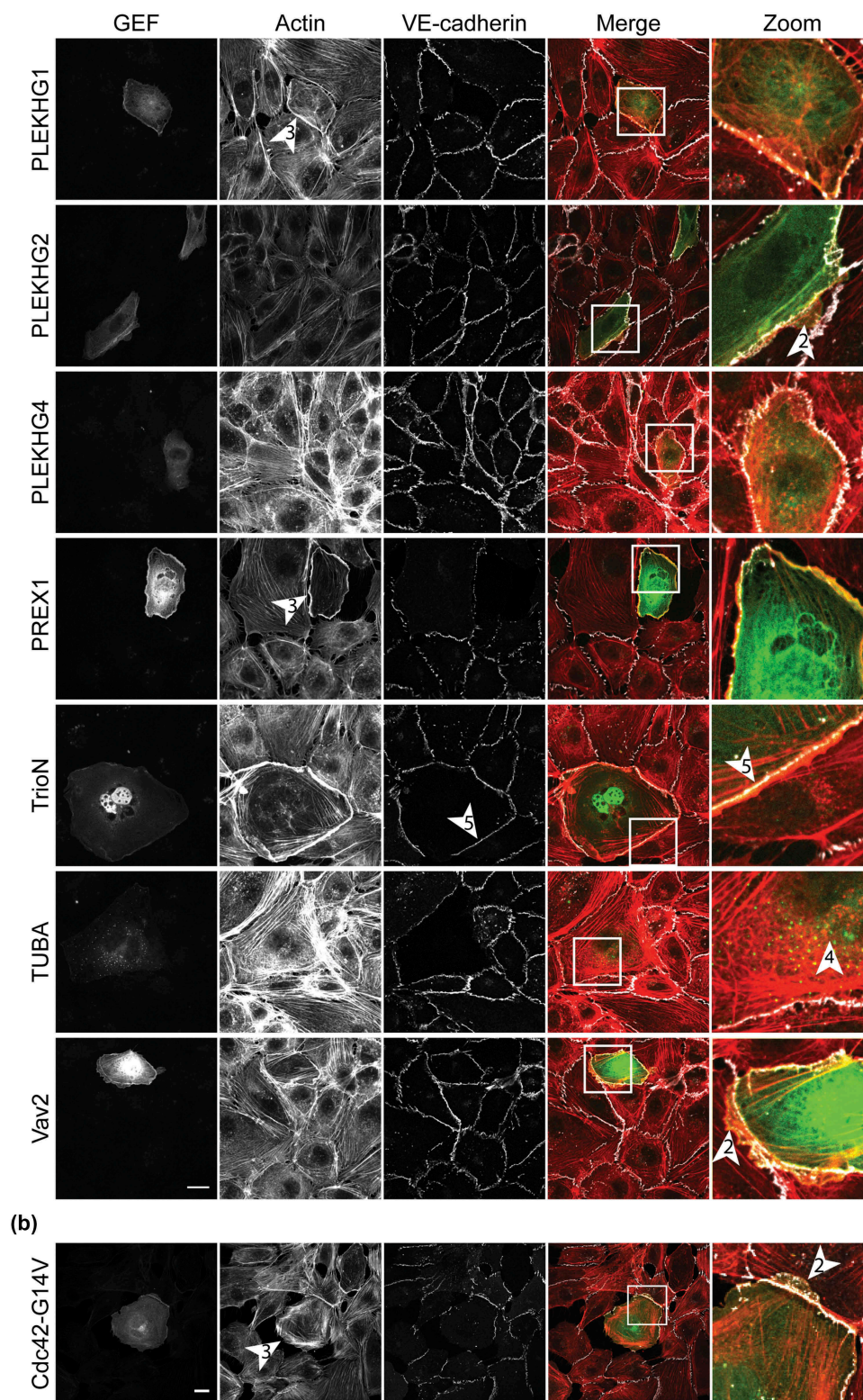


Figure 2b. (Continued)

interval (Figure 4(c,d)). Based on arbitrarily set cut-off values we have defined three levels of activation of Cdc42 i) no Cdc42 activation; Asef2, β -Pix, α -Pix and FGD5 ii) intermediate activation; TUBA, Vav2, PLEKHG4, ITSN2, TrioN, SGEF and ITSN1, and iii)

strong activation; PLEKHG2, FGD1, PLEKHG1 and PREX1. A similar categorization for Rac1 defines the GEFs with i) no Rac1 activation; FGD1, Asef2, β -Pix, α -Pix, FGD5 and ITSN1, ii) intermediate activation; PLEKHG1, PLEKHG4, SGEF, ITSN2, PLEKHG2 and

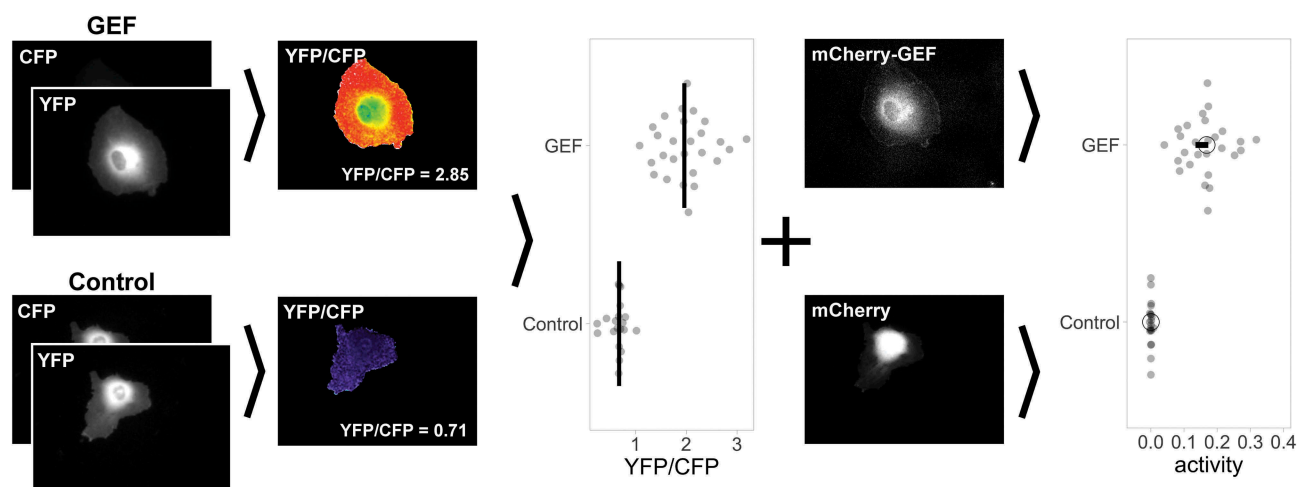


Figure 3. Workflow of GEF-mediated Cdc42 activation measurements in single ECs.

Data points are part of an actual experiment included in this paper. ECs were transiently transfected with the YFP/CFP-based Cdc42-FRET sensor, and either C1-mCherry- or a mCherry-GEF. YFP and CFP images were acquired to generate the YFP/CFP ratio images and to quantify these values per cell. The median YFP/CFP value is depicted in the graphs as a vertical line. Subsequently, the mCherry intensity was used to convert the YFP/CFP ratio data into values of ‘relative activity’. The median activity is depicted as a circle and the 95% confidence interval determined by bootstrapping is indicated as a horizontal bar. For a detailed explanation see supplementary Figure S1.

TUBA, and iii) strong activation; Vav2, PREX1 and TrioN (Figure 4(c,d)).

To examine whether Cdc42 activity can be linked to a quantifiable phenotype, we determined the cell area for each of the conditions (Supplemental Figure S2). There is substantial variability in the cell area, with Asef2, SGEF and Vav2 showing the largest increase in cell area. Of these three RhoGEFs, Asef2 does not show any activity in our biosensor assay, SGEF has moderate effects on both Cdc42 and Rac1 and Vav2 only on Rac1. Hence, no obvious relation between cell area and biosensor activity was observed.

Overall, these data show distinct GEF-induced Cdc42 and Rac1 activation profiles in live ECs. Different GEFs can be divided into low-, medium-, and high activators, with a differential preference for Cdc42 or Rac1 GTPases.

TIAM1 exclusively activates Rac1, and not Cdc42

As shown in Figure 4, PREX1, TrioN and Vav2 all, to some extent, activate Cdc42. Previous literature, however, mainly describes these GEFs as Rac1 activators. To test the specificity and discriminative power of our assay, we used the GEF TIAM1 as an additional negative control. Based on *in vitro* data [13], TIAM1 is highly selective, showing high GEF activity towards Rac1, but not towards Cdc42. Applying the same strategy as described in Figure 3, the catalytic domain of TIAM1 was used to study the effect on Cdc42 or Rac1. Ectopic expression of mCherry-TIAM1, combined with the Cdc42 FRET sensor, did not show Cdc42 activation based on the YFP/CFP ratio (Figure 5(a)) and also its relative activity was near

the control value (Figure 5(c)). In contrast to Cdc42, strong effects were observed when the Rac1 sensor was used in combination with TIAM1. Both the YFP/CFP ratios, as well as the relative activity, were strongly increased relative to the control (Figure 5(b,d)). These data suggest that the Cdc42 biosensor is not sensitive for Rac GEFs and that induction of Rac1 activity does not (indirectly) result in Cdc42 activation in endothelial cells.

Collectively, our data demonstrate that the Cdc42 and Rac1 biosensors report with high selectivity on GEF activity in a cellular context.

Catalytic GEF domains induce differential Cdc42 activation patterns

As can be inferred from the protein domain structures in Figure 1, the GEFs of interest belong to the Dbl family (containing a DH and PH domain). The activity that we have measured for the FL GEFs (Figure 4) is a basal activity determined by the combined role of all the domains that are present. Previous studies have demonstrated that the DH domain is responsible for the catalytic activity towards their preferred targets [4,10,13]. The PH domain that is adjacent to the DH domain in the majority of GEFs has a less clearly defined role. Finally, domains beyond the DHPH tandem can have diverse regulatory roles, including localization, autoinhibition, protein–protein or protein–lipid interactions. To study the role of the catalytic unit in more detail, we selected a number of GEFs to examine the activity of the DH domain and the role of the PH domain.

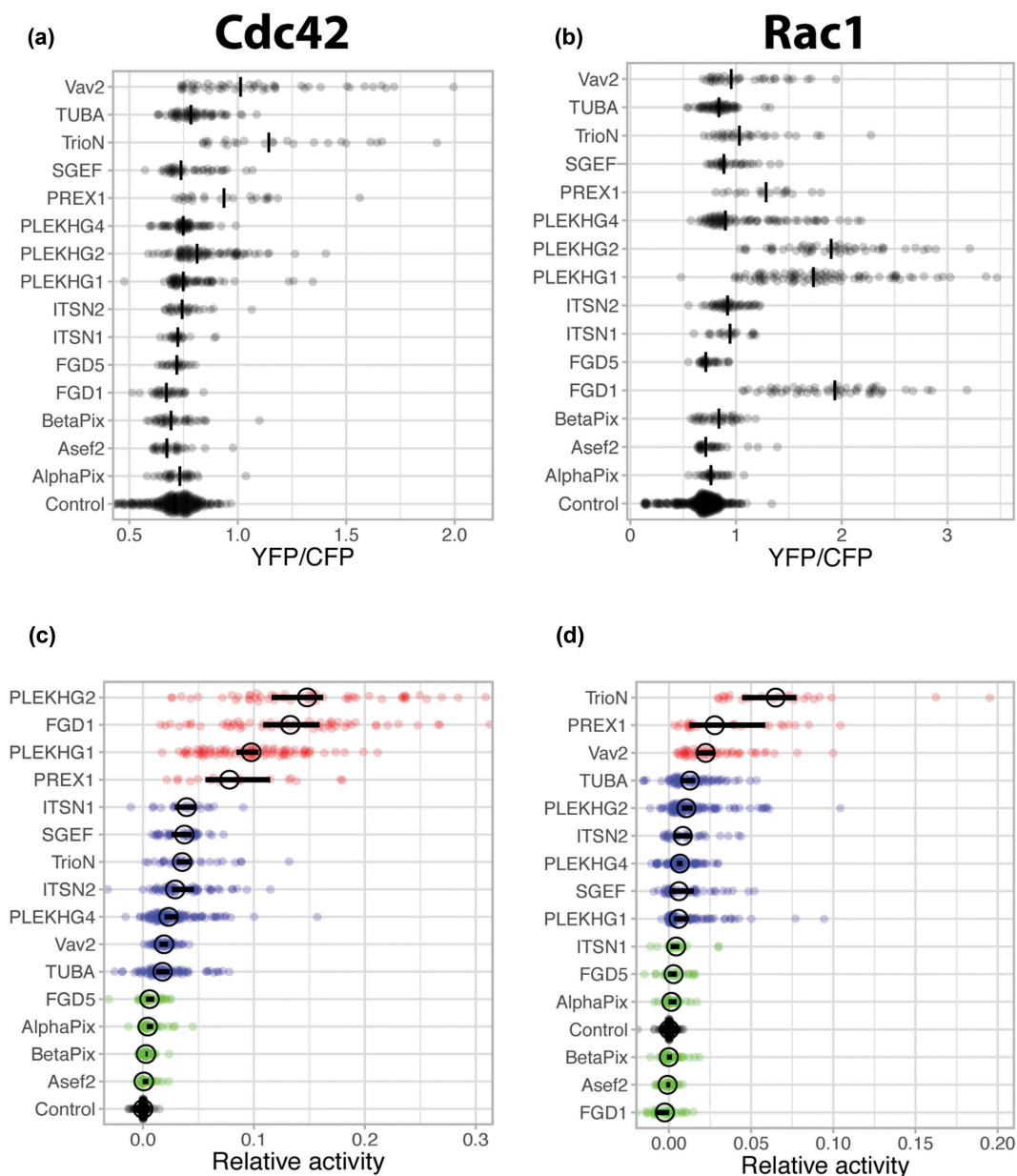


Figure 4. Ectopic expression of GEFs induce distinct Cdc42 and Rac1 activation patterns.

(a) Average YFP/CFP ratios of ECs that were transiently transfected with the Cdc42-FRET sensor and either C1-mCherry (Control, $n = 296$) or mCherry-fused GEFs (α -Pix $n = 30$, Asef2 $n = 33$, β -Pix $n = 38$, FGD1 $n = 55$, FGD5 $n = 29$, ITSN1 $n = 20$, ITSN2 $n = 49$, PLEKHG1 $n = 88$, PLEKHG2 $n = 70$, PLEKHG4 $n = 82$, PREX1 $n = 18$, SGEF $n = 33$, TrioN $n = 31$, TUBA $n = 52$ and Vav2 $n = 36$). **(b)** Average YFP/CFP ratios of ECs that were transiently transfected with the Rac1 FRET sensor and either C1-mCherry (Control, $n = 271$) or mCherry-fused GEFs (α -Pix $n = 33$, Asef2 $n = 31$, β -Pix $n = 38$, FGD1 $n = 31$, FGD5 $n = 22$, ITSN1 $n = 21$, ITSN2 $n = 28$, PLEKHG1 $n = 64$, PLEKHG2 $n = 81$, PLEKHG4 $n = 61$, PREX1 $n = 24$, SGEF $n = 41$, TrioN $n = 24$, TUBA $n = 61$ and Vav2 $n = 50$). **(c&d)** The relative activity calculated from the YFP/CFP ratios and the mCherry intensities quantified from single cells. The median and 95% confidence interval are indicated by a circle and horizontal bar, respectively. The green, blue and red colours define no activation, intermediate activation and strong activation, respectively. Online, interactive plots are available for [panel C](#) and [panel D](#).

In total eight GEFs from all three levels of Cdc42 activation (weak, intermediate, strong) were selected, including FGD1, FGD5, ITSN1, ITSN2, PLEKHG1,

PLEKHG2, PLEKHG4 and PREX1. Corresponding GEF DHPH domain alignments (acquired from ClustalW) highlight the amino acid sequence homology

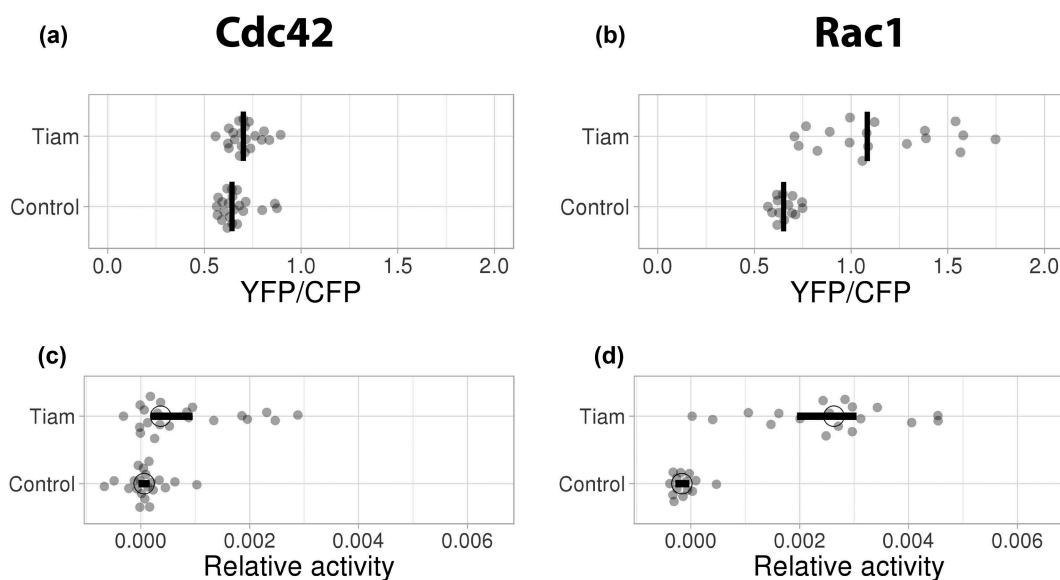


Figure 5. Ectopic expression of TIAM exclusively activates Rac1.

(a) YFP/CFP ratios of ECs that were transiently transfected with the Cdc42 FRET sensor and either C1-mCherry (Control, $n = 22$) or mCherry-TIAM ($n = 21$). **(b)** YFP/CFP ratios of ECs that were transiently transfected with the Rac1 FRET sensor and either C1-mCherry (Control, $n = 14$) or mCherry-TIAM ($n = 18$). **(c)** The relative activity observed with the Cdc42 sensor based on the YFP/CFP ratios shown in panel A and mCherry intensity. **(d)** The relative activity observed with the Rac1 sensor based on the YFP/CFP ratios shown in panel B and mCherry intensity. In C and D the median and 95% confidence interval are indicated with a circle and bar, respectively.

between these proteins (Figure 6). We generated mCherry-fused DH, and DHPH constructs. Since it has been shown that recruitment of a GEF to the plasma membrane is sufficient to increase Rho GTPase activity, we also made variants with a plasma membrane targeting signal from Lck.

We tested to what level the different DH/DHPH constructs activated Cdc42, relative to the corresponding full length (FL) GEFs. Distinct activation patterns were observed for the GEFs of interest (Figure 7(a–h) and Supplemental Figure S3). PLEKHG2 and PREX1 showed pronounced Cdc42 activation by the FL protein, while the DH/DHPH constructs hardly showed Cdc42 activation (Figure 7(a,h) and Supplemental Figure S3(f,h)). In contrast to the average YFP/CFP ratio plots, a pronounced effect was observed for the relative activities of three of the FGD1 truncation constructs; DH, DHPH and Lck-DHPH, respectively (Figure 7(a) and Supplemental Figure S3(a)). We think that the relative activity measure is a better indicator of activating the potential of a GEF, since it takes the expression level of the GEF into account.

A difference in YFP/CFP ratio and activity value was not observed for PLEKHG2 and PREX1 (Figure 7(f,h) and Supplemental Figure S3(f,h)). For the weak activator FGD5, neither the average YFP/CFP ratio, nor the activity values were affected in any of the conditions (Figure 7(b) and Supplemental Figure S3(b)). Relative to the FL and the DH constructs, the DHPH constructs induced high

YFP/CFP ratio increases for ITSN1, ITNS2, PLEKHG1 (Supplemental Figure S2(c–e)). A different pattern was observed in the corresponding relative activities. Here the effect of the DHPH truncation constructs was less pronounced relative to the FL constructs (Figure 7(c–e) and Supplemental Figure S3(c–e)). Finally, the catalytic PLEKHG4 constructs induced moderate increases in Cdc42 activation as compared to the FL PLEKHG4 (Figure 7(g) and Supplemental Figure S3(g)).

In summary, for FGD1, ITSN1, ITSN2 and PLEKHG1 different patterns were observed when comparing average FRET ratios and corresponding relative activities. Together, our data show that catalytic domains of different GEFs, show unanticipated and distinct Cdc42 activation profiles.

Discussion

Over the past years, more than 80 GEFs have been identified and they have been shown to be involved in a variety of functions and signalling networks. This study focusses on a selection of Dbf-family RhoGEFs, that may signal towards Cdc42 in the endothelium, including α -Pix, Asef2, β -Pix, FGD1, FGD5, ITSN1, ITSN2, PLEKHG1, PLEKHG2, PLEKHG4, PREX1, SGEF, TrioN, TUBA and Vav2. Fluorescent-labelled versions of these GEFs provide new insights regarding the localization of these proteins in primary human ECs. We furthermore implement a robust

FGD1	364	SVELTVQKVFHIANELLQTEKAYVSRLLHLLDQVFCARLLEEAR-----NRSSF PADVWH
FGD5	884	THKVEGQSRALVIAQELLSSEKAYVEMLQHLNLD FHGAVMRALD DMDHEGRDTLARELELR
ITSN1	1229	DMLTPTERKROGYI HELIVTEENYVNDLQLVTEI FQKPLMESE-----LL TEKEVA
ITSN2	1200	DTMQPIERKRQGYI HELIQTEERYMADLQLVVEV FQKRMAESG-----FL TEKEVA
PLEKHG1	105	SATSPKLLYVDRVVQEILETERTYVQDLKSI VEDYLD CIRDQT-----KLP LGTEERS
PLEKHG2	94	IPGSARPSRLERVA REIVETERAYVRDLRSI VEDYLG PLDGG-----VLGLSVEQVG
PLEKHG4	723	SSDPRSLNRLQLVLAEVATEREYVRALEYTMEN YFPEDRDP-----VPQGLRGQRA
pRex1	53	-----VLNELGTERDYVGTLRFLQSAFLHRIRQNVADS---VEKGLTEENVK
		* : : * . * : * . : : :
FGD1	419	GIFSNICSIYCFHQQFLLPEL--E KRMEEDRYP RIGDILQKLA PFLKMYGEYVKNFDR
FGD5	944	QGLSELPAIHDLH-QGILEEL--E ERLSNWESQQKVADVFLARE QGFDHATHI LQFDRY
ITSN1	1280	MI FVNWKE LIMCNI KLLKALRVRK KMSGKMPVKMIGDILSAQL PHMQPYIRFC SRQLNG
ITSN2	1251	LI FVNWKE LIMSNT KLLKALRVRKKTGGEKMPVQMI GDILAAEL SHMQAYIRFC SCQLNG
PLEKHG1	158	ALFGNIQDIYHFNS E-LLQDLE--NCE---NDPVAIAECFVSKS EEFHIYTYQC TNYPRS
PLEKHG2	147	TLFANIEDIYEFSS E-LLEDLE--NSS---S-AGGIAECFVQRS EDFDIYTYLCMNYPS
PLEKHG4	776	HLFGNLEKLRDFHC HFFLRELE--ACT---RHPPRVAYAF LRHRVQFGMYALLQEL ARACGG
pRex1	98	VLFNSNIEDILEVHKDFLAAL E--YCLHPEPQSQHELGNVFLKFKDKFCVVEEYK SNHEKA
		: : : . : : : : : : : .
FGD1	477	VELVNTWTERSTQF KVI IH-EVQKEEACGNLT LQHMMLEPVQRI PRYELLKKDY LKLP
FGD5	1001	LGLLSENCLHSPRLAAAVR-EFEQ SVQGGSQ TAKHLLRVVQRL FQYQVLLTDY LNNLC
ITSN1	1340	AALIQQKTDEAPDF KEFVK-RLAMDPRCKGMPLS SFILKPMQVRV TRYPLI IKNI LENTPE
ITSN2	1311	AALQQKTDEDTDF KEFLK-KLAS DPRCKGMPLS SFLLKPMQRI TRYPLLIRSI LENTPE
PLEKHG1	212	VAVLTECMRNKI LAKFFRE---RQETLKHSLPLG SYLLKPVQRI LKYHLLLHEI ENHLDK
PLEKHG2	200	LALLRELSLSPPAALWLQE---RQAQLRHSLPLQ SFLLKPVQRI LKYHLLLQEL GKHWAE
PLEKHG4	831	DALMSS-----YGH TFFKD---KQALGDHLDLA SYLLKPIQRMGKYALLLQEL ARACGG
pRex1	156	LRLVLELNKIPTVRAFLLS CMLLG GRKTTDI PLE GYLLSPIQRI CKYPLLLKELAKRTPG
		: : : : : * : * : * : * : : .
FGD1	536	--GSPDSKDAQKSL ELIATAAEHS NAAIRKMERMHKLLKVYELLGEE--DIVS -----
FGD5	1060	--DSEYDNTQ GALSLISKVTD RANDSMEQGENL QKLVHIEHSVRGQ--DLLQ -----
ITSN1	1399	--NHPDHSHLKHAL EKAEELCSQVNEGVREKENS DRLEWIQAHVQCEGLSEQLV FNSVTN
ITSN2	1370	--SHADHSSLKLAL ERAEELCSQVNEGVREKENS DRLEWIQAHVQCEGLAEQLI FNSLTT
PLEKHG1	269	--DTEGYDVVLD AI DTMQRVAWHI NDMKRKHEHA VRLQEIQSLL TNWKPDLTYS-----
PLEKHG2	257	GPCTGGREMVEEAI VSMATAVAWYI NDMKRKQEHAA RLQEVQRRLGGWTGPELSAF-----
PLEKHG4	883	--PT-----QEL SALS REAQS LVHFQ---LRHGNL LAMDAIQG-----CDVNLKEQ-----
pRex1	216	--KHPDHPAVQSALQAMKTVCSNI N ETKRQMEKLEALEQLQSHI EGWEGSNLT D-----
		: : : : : : : : : :
FGD1	586	--PTKELIKEGHIL KLSAK--NGT QDRYLILFN DRLLYCVPRLLRLLGQKFSVRARID--
FGD5	1110	--PGREFLKEGTLMKVTGK--NRRP--RHLFLMNDVLLLYTPQKD--GKYRLKNTLA--
ITSN1	1457	CLGPRKFLHSGKLY KAKSN-----KELYGFLNDFLLLTQITKPLG--SSGTDKVFSPKS
ITSN2	1428	CLGPRKLLHSGKLY KTKSN-----KELHGFLNDFLLLTVMVKQFAVSSGSEKLFSSKS
PLEKHG1	322	----GELVLEGTFR IQRA-----KNERTLFLFDKLLLIITKRRD-----
PLEKHG2	312	----GELVLEGAFRGGGGGPRLRGGERLFLF S RMLLVAKRRG-----
PLEKHG4	924	----GQLVRQDEFVVRTGR----HKS VRRIFLFE ELLLF SKPRH GPTG-----
pRex1	268	--ICTQLLLQGTLLKISAG--NI--QERAFFLFDNLVYCKRKS RVTGSKKSKTRKTS-I
		: : : . : . : : : * : * : *
FGD1	640	-----VDGMELKESSNLNMP-----RTFLV---S-GKQRSLELQARTEE
FGD5	1159	-----VANMKVSRPVMEKVP-----YALKI---E-TSESCLMLSASSCA
ITSN1	1510	NLQYKMYKTPIFLNEVLVKLPDTPSGD-----EPIFHI---S-HIDRVYTLRAESIN
ITSN2	1482	NAQFKMYKTPIFLNEVLVKLPDTPSSD-----EPVFHI---S-HIDRVYTLRDTNIN
PLEKHG1	356	--DTFTYKAHILCGNMLMVEVI-PKEP-----LSFSVFHYK-NPKLQHTVQAQSQ
PLEKHG2	352	--LEYTYKGHIFCCNLSVS-ES-PRDP-----LGFKVSDLT-IPKRRHLLQAKNQE
PLEKHG4	964	-VDTFAYKRSFKMADLGLTECC-GNSN-----LRFELIWFRRRKARDTFVLQASSLA
pRex1	321	NGSLYIFRGRINTEVMEVENVEDGTADYHSNGYTVTNGWKIHN-T-AKNKWFVCMAKTAE
		: : : : : : : : : :
FGD1	675	EKKDWVQAINS-----
FGD5	1194	ERDEWYGCLSR-----
ITSN1	1558	ERTAWVQKIKAASELYIETEKKK
ITSN2	1530	ERTAWVQKIKAASEQY-----
PLEKHG1	403	DKRLWVHLKRLILEN-----
PLEKHG2	398	EKRLWIHCLQRLFFEN-----
PLEKHG4	1013	IKQAWTADISHLLWRQ-----
pRex1	379	EKQKWLDAIIREREQR-----
		: * :

Alignment of GEF DH/PH domains. ITSN1, ITSN2, PLEKHG1, PLEKHG2, PLEKHG4 and PREX1. Numbers indicate corresponding amino acid position of the FL protein. Dark grey represents the DH domain, light grey represents the PH domain. * represents single, fully conserved residue, : represents conserved residues between groups of strongly similar properties, . represents conserved residues between groups of weakly similar properties.

FRET-based and live-cell assay, to measure and quantitatively compare GEF-mediated activation of Cdc42. This demonstrates differential activation patterns, induced by FL GEFs or their isolated DH/DHPH domains.

So far, most of these selected GEFs have not been studied in the endothelium. We visualize these proteins in ECs by generating mTq2-labelled GEF constructs and reveal diverse localizations and different GEF-

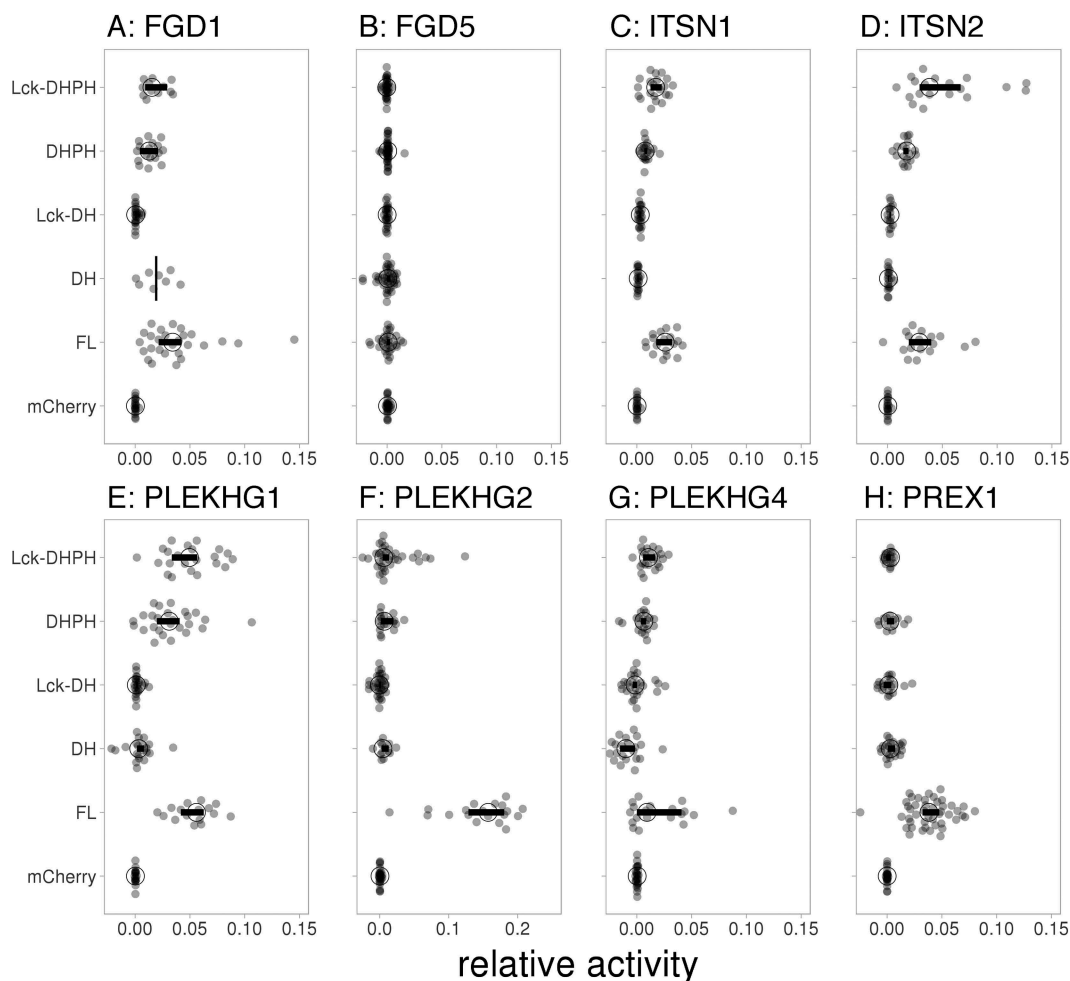


Figure 7. Catalytic GEF domains induce distinct Cdc42 activation profiles. For each of the indicated GEFs the relative activity of membrane-targeted (Lck) Lck-DHPH, soluble DHPH, Lck-DH, soluble DH or full-length (FL) on the Cdc42 biosensor was quantified relative to the control (mCherry). The median activity and 95% confidence intervals are indicated with a circle and a horizontal bar, respectively (except for the ‘DH’ condition of FGD1, where only the median is indicated due to low sample size). The corresponding YFP/CFP data are represented in Supplemental Figure S3.

induced phenotypes. Although these localization studies are descriptive, specific phenotypes (e.g. FGD1-induced membrane protrusions) hint towards the activation of Cdc42. However, the cell area, taken as a quantitative phenotype, did not reveal an obvious connection between activity and this phenotype.

Integrating GEF overexpression with our single-cell FRET strategy, allowed us to generate large datasets of GEF-induced activation of Cdc42 or its close homologue Rac1. To relate the observed activities to GEF expression levels, we performed Theil–Sen estimation analyses, generating slope values for each individual datapoint. The outcome of the analysis, the relative activity, reflects the intrinsic, basal activity of the GEF. Based on this strategy, we observe differential activation profiles for Cdc42 and Rac1, underscoring the specificity of this assay. Of note, the amplitude differences in YFP/CFP ratio between Rac1 and Cdc42 biosensors are most likely the result of a higher

dynamic range of the Cdc42-FRET sensor. This technical limitation still allows us to compare trends in Cdc42 and Rac1 activation while comparisons of actual YFP/CFP ratios and absolute activity values are not straightforward.

The global Rho GTPase activity that we quantified may mask local effects. These aspects need to be addressed in follow-up studies, since it is known that the localization of the Rho GTPase activity can be an important determinant of the biological effect [27]. This may also explain the lack of a relation between phenotypes and activity that we document here. Therefore, future studies may use higher resolution imaging, i.e. by using some sort of optical sectioning, or other types of biosensors that allow for increased spatial resolution.

We chose an over-expression strategy since it enables us to select cells that express the GEF of interest and quantify its relative concentration. Over-expression studies in general, should be interpreted with caution. First,

the levels of the GEF are strongly elevated and may, therefore, exceed levels that are physiologically relevant. Moreover, the activity that is observed can be a consequence of the unbalanced presence of regulators. Finally, the activity may be an indirect consequence of the over-expressed RhoGEF, for instance through endogenous proteins that in turn may activate the Rho GTPase or the induction of gene expression leading to elevated activity. In our study, we evaluated the activity of RhoGEFs that are relevant for endothelial biology and overexpressed these in endothelial cells. However, a RhoGEF that displays a strong phenotype or effects on a Rho GTPase biosensor does not necessarily have a role in endothelial signalling. A downregulation strategy would be better suited to identify regulators that are critical for basal Cdc42 activity under physiological conditions. However, we observed that the Cdc42 activity is low in unperturbed endothelial cells (Figure 4(a)). As a consequence, we will not be able to observe a decrease in Cdc42 activity with the FRET probe.

The strongest Cdc42 activators comprise FGD1, PLEKHG1 and PLEKHG2. The lack of FGD1-induced Rac1 activation underscores the specificity of FGD1-induced Cdc42 activation. This is well in line with previous studies that characterized FGD1 as a Cdc42 GEF involved in faciogenital dysplasia, a human disease that affects skeletogenesis [28,29]. We observe most prominent Rac1 activation for TrioN, PREX1, Vav2 and TIAM1, in line with previous studies which defined these as Rac1 GEFs [13]. We also observed elevated Cdc42 activation for PREX1, and to some extent for TrioN and Vav2. The activity of PREX1 towards Cdc42 has been observed using purified components [13], but not in cellular context [30]. Whether the activation of Cdc42 by PREX1 is direct remains to be determined. It could, for instance, be caused indirectly by the PREX1-induced expression or recruitment of another Cdc42 activating RhoGEF. The Cdc42 activation is unlikely to be mediated by Rac1 activity, since the activation of Rac1 by Tiam did not result in Cdc42 activation. While FGD5, ITSN1 and TUBA have already been linked to Cdc42 activation [31–33], our approach only detects moderate signalling towards Cdc42. However, it should be noted that our approach measures basal activity of the GEFs. The activity may be increased by signalling or affected by the binding of accessory/scaffolding proteins. A limitation of our assay is that we may miss the effects of endogenous accessory proteins due to over-expression of the GEFs. Additionally, In ECs, we observe that ITSN1 and TUBA primarily localize at vesicles. But, it is unexplored whether Cdc42 can get activated at these localized structures.

GEF activities of the full-length proteins can be influenced by auto-inhibitory domains [34], protein–protein interactions and by phosphorylation of specific residues [35]. Although FL GEF studies may appear physiologically the most relevant, the use of isolated GEF domains limits complexity. A selection of our catalytic constructs induces elevated Cdc42 activation, most clearly for the membrane-linked, DHPH constructs of ITSN1, ITSN2 and PLEKHG1 and to some extent for FGD1 and PLEKHG4. This suggests that the respective DHPH domains are functional and also proposes these GEFs as interesting candidates in recruitment- and/or optogenetic systems, to locally induce Cdc42 activation at the plasma membrane. We [36], and others [37,38], have already demonstrated the value of these approaches in biological systems. Interestingly, we observe distinct trends in activation when comparing YFP/CFP ratio- and corresponding activity analyses. Compared to DHPH domains, FL GEFs exhibit higher ‘relative activity’. This implies that the activity of the GEFs is controlled by domains other than the DHPH domains.

Previously, we observed with a similar strategy that the PH domain of p63RhoGEF has an autoinhibitory role and that the isolated DH domain has high activity towards RhoA [36]. However, we did not find a similar role for the PH domain in any of the GEFs that we analysed. Strikingly, the isolated DH domains (with the exception of the DH domain of FGD1) did not show any activity in a cellular context. It appears that the PH domains of the Cdc42 GEFs that we selected have a stimulatory rather than inhibitory role.

In contrast to the previous-mentioned GEFs, effects of DHPH domains of FGD5, PLEKHG2 and PREX1 are either small or absent. Although we carefully designed the constructs to capture the entire domain (i.e. not disrupting any secondary structures) it is unclear whether these truncated protein domains are correctly folded and functional. This is a general limitation of expressing isolated protein domains in cells. When no activity is observed it does not provide evidence that the protein domain does not have activity in the full-length protein. To address the functionality, the activity of the isolated (fusion) protein needs to be examined and compared to the cell-based assays. This is a labour-intensive undertaking, but it may ultimately be required to draw solid conclusions.

In conclusion, this study provides new insights regarding GEF-mediated Cdc42 activation in live, primary human ECs. Our FRET-based GEF screening method identifies FL PLEKHG2, FGD1, PLEKHG1 and PREX1 as prominent Cdc42 activators. Additionally, catalytic domains of ITSN1, ITSN2 and PLEKHG1 behave as

potential activators for local-induced Cdc42 activation at the plasma membrane. Overall, these findings point to novel potential Cdc42-related (signalling) processes in the endothelium.

Methods

Plasmids

FL GEFs

For Asef2 (kind gift from D. Webb) and PREX1 (kind gift from H.C. Welch), mTq2 and mCherry were amplified by PCR. PCR products (inserts) and vectors were cut with restriction enzymes. Next, digested products were ligated to generate mTq2- and mCherry-GEF fusions.

For β -Pix and TrioN (kind gifts from J. van Buul), vectors and GEF constructs were cut with restriction enzymes. Next, digested products were ligated to generate mTq2- and mCherry GEF fusions.

For α -Pix (kind gift from J.L. Zugaza), FGD1 (kind gift from M. Hayakawa), FGD5 (kind gift from W.J. Pannekoek), ITSN1 (obtained from

Addgene, plasmid #47395), ITSN2 (kind gift from I. G. Macara), PLEKHG1 (kind gift from K. Mizuno), PLEKHG2 (kind gift from H. Ueda), PLEKHG4 (kind gift from D. Manor), SGEF (kind gift from J. van Buul), TUBA (kind gift from L.J.M. Bruurs) and Vav2 (obtained from Addgene, plasmid #14554), GEFs were amplified by PCR. PCR products (inserts) and vectors were cut with restriction enzymes. Next, digested products were ligated to generate mTq2- and mCherry-GEF fusions.

Corresponding PCR primers, restriction enzymes, and cloning products are listed in Table 1. The plasmids of the mCherry fusions are available from Addgene.org with these plasmid numbers 129609: mCherry-AlphaPix, 129610: mCherry-Asef2, 129611: mCherry-BetaPix, 129612: mCherry-FGD1, 129613: mCherry-FGD5, 129614: mCherry-ITSN1, 129615: mCherry-ITSN2, 129616: mCherry-PLEKHG1, 129617: mCherry-PLEKHG2, 129618: mCherry-PLEKHG4, 129619: mCherry-PREX1, 129620: mCherry-SGEF, 129621: mCherry-TrioN, 129622: mCherry-TUBA and 129623: mCherry-Vav2

Table 1. Generation of FL mTq2/mCherry-GEF constructs. RE = restriction enzyme, Fw = Forward primer, Rv = Reverse primer. Restriction sites are underlined in the primer sequences. Restriction sites for Asef2, PREX1 and SGEF are not present in the Fw primer.

PCR primers	RE1/RE2	Product(s)
Fw: 5'- gagatcgaattccatgacgcaaaatggaagtcac -3' Rv: 5'- gagatcggatccttattatggaagaattgaggtcttg -3'	EcoRI BamHI	C1-mTq2/mCherry- α -Pix
Fw: 5'- aggtctatataagcagagc -3' Rv: 5'- gagatcctcgagccatctgagtcggacttg -3'	AgeI XhoI	C3-mTq2/mCherry-Asef2
- -	AgeI BsrGI	C1-mTq2/mCherry- β -Pix
Fw: 5'- gagatcagatctcatgcccaccgagtc -3' Rv: 5'- gagatcgaattcttaggtctgtctcgggtctg -3'	BglII EcoRI	C1-mTq2/mCherry-FGD1
Fw: 5'- gagatcagatctatggtcaggggtccgaag -3' Rv: 5'- gagatcgaattcttataacacactcgcacatctcc -3'	BglII EcoRI	C1-mTq2/mCherry-FGD5
Fw: 5'- gagatcctcgagccgctcagttccaacacttttg -3' Rv: 5'- gagatcggtagctctacggtctcaaaactgc -3'	XhoI Acc65I	C1-mTq2/mCherry-ITSN1
fw: 5'- gagatcgtcgacgctcagttcccagctatg -3' rv: 5'- gagatcctagattacagagaggttttctcaaaaag -3'	Sall XbaI	C1-mTq2/mCherry-ITSN2
Fw: 5'- gagatcctcgagccgagctctctgtagtgaccgac -3' Rv: 5'- gagatcgaattcttaagcaagctgctggaactg -3'	XhoI EcoRI	C1-mTq2/mCherry-PLEKHG1
Fw: 5'- gagatcagatctatgctgagggagccc -3' Rv: 5'- gagatcgaattctcacatgtggaaggggg -3'	BglII EcoRI	C1-mTq2/mCherry-PLEKHG2
Fw: 5'- gagatcctcgagccgaagggcccctggaga -3' Rv: 5'- gagatcggtagcttagacacagggtaagtcctcc -3'	XhoI Acc65I	C1-mTq2/mCherry-PLEKHG4
Fw: 5'- aggtctatataagcagagc -3' Rv: 5'- gagatcgaattcggaaagcttgagc -3'	AgeI EcoRI	C3-mTq2/mCherry-PREX1
Fw: 5'- aggtctatataagcagagc -3' Rv: 5'- gagatcgaattcggaaagcttgagc -3'	AgeI EcoRI	C1-mCherry-SGEF
- -	AgeI BsrGI	C1-mTq2/mCherry-TrioN
Fw: 5'- gagatcgtcgacatggaggctggtcagtg -3' Rv: 5'- gagatcctagattaggtgactcgggtttgagc -3'	Sall XbaI	C1-mTq2/mCherry-TUBA
Fw: 5'- gagatcctcgagccatggagcagtggtggcagac -3' Rv: 5'- gagatcggtagcttactgagtcctctcttc -3'	XhoI Acc65I	C1-mTq2/mCherry-Vav2

DH(PH) truncation constructs

DH and DHPH domains of FGD1, FGD5, ITSN1, ITSN2, PLEKHG1, PLEKHG2, PLEKHG4 and PREX1 were amplified by PCR, using the same template constructs as for the cloning of the FL constructs. Next, PCR products (inserts) and vectors were cut with restriction enzymes. Finally, inserts were ligated into vectors to generate for each GEF mCherry-DH, Lck-mCherry-DH, mCherry-DHPH and Lck-mCherry-DHPH constructs. An overview of PCR primers and restriction enzymes are listed in Table 2.

Others

Cdc42-G14V (cDNA.org) was amplified by polymerase chain reaction (PCR), using a forward primer (BsrGI site in uppercase): gCTGTACAagtcctatgcagacaattaagtgtg and reverse primer 3'-pcdna: gtcgaggctgatcagcgg. PCR product was digested with BsrGI and XbaI and inserted in a clontech style backbone. The Rac1 FRET sensor [25] and Cdc42-FRET sensor [26,39] were as published in the cited references.

Immunofluorescence

Actin-stain 555 Phalloidin was from Cytoskeleton, a monoclonal antibody (mAb) Mouse anti-VE-cadherin/CD144 AF647 was purchased from BD Pharmingen

HUVEC culture and transfection

Primary HUVECs, purchased from Lonza (Verviers, Belgium), were seeded on fibronectin (FN)-coated culture dishes and grown in EGM2 medium (supplemented with SingleQuotes (Lonza)). HUVECs (at passage #4 or #5) were transfected with 2µg plasmid DNA, using a Neon transfection system (MPK5000, Invitrogen) and a corresponding Neon transfection kit (Invitrogen) that generates a single pulse at 1300 V for 30 ms. After microporation, HUVECs were seeded on FN-coated glass coverslips.

Confocal imaging

Transfected HUVECs were grown to a monolayer, washed in PBS (1mM CaCl₂ and 0.5 mM MgCl₂) and fixed in a PBS solution (1mM CaCl₂ and 0.5 mM MgCl₂) with 4%

Table 2. Generation of (Lck-)mCherry-DH(PH) GEF constructs. RE = restriction enzyme, Fw = Forward primer, Rv = Reverse primer. Restriction sites are underlined in the primer sequences.

PCR primers	RE1/RE2	Products
Fw: 5'- gagatcagatcttctgtggagctgactgtgc -3' Rv: 5'- gagatcgaattcttaggctatcagctcacaagac -3'	BgIII EcoRI	(Lck-)mCherry-FGD1-DH
Fw: 5'- gagatcagatcttctgtggagctgactgtgc -3' Rv: 5'- gagatcgaattcttaggaattgatggcctggac -3'	BgIII EcoRI	(Lck-)mCherry-FGD1-DHPH
Fw: 5'- gagatcagatctaccacaaggtggaagg -3' Rv: 5'- gagatcgaattcttagctgtggcacgctgtg -3'	BgIII EcoRI	(Lck-)mCherry-FGD5-DH
Fw: 5'- gagatcagatctaccacaaggtggaagg -3' Rv: 5'- gagatcgaattcttaggctctgctcagacagcc -3'	BgIII EcoRI	(Lck-)mCherry-FGD5-DHPH
Fw: 5'- gagatcagatctgatattgaccccaactg -3' Rv: 5'- gagatcgaattcttattcactctgggaac-3'	BgIII EcoRI	(Lck-)mCherry-ITSN1-DH
Fw: 5'- gagatcagatctgatattgaccccaactg -3' Rv: 5'- gagatcgaattcttactcttttctcagctctctatgtag -3'	BgIII EcoRI	(Lck-)mCherry-ITSN1-DHPH
Fw: 5'- gagatcagatctgacacaatgcagccaattg -3' Rv: 5'- gagatcgaattcttactcttagctgagagcagctcctc -3'	BgIII EcoRI	(Lck-)mCherry-ITSN2-DH
Fw: 5'- gagatcagatctgacacaatgcagccaattg -3' Rv: 5'- gagatcgaattcttagtactgctcagagccg -3'	BgIII EcoRI	(Lck-)mCherry-ITSN2-DHPH
Fw: 5'- gagatcagatcttcggccacgagc -3' Rv: 5'- gagatcgaattcttagctattgatgcccaggc -3'	BgIII EcoRI	(Lck-)mCherry-PLEKHG1-DH
Fw: 5'- gagatcagatcttcggccacgagc -3' Rv: 5'- gagatcgaattcttagttctcagaatcagctctc -3'	BgIII EcoRI	(Lck-)mCherry-PLEKHG1-DHPH
Fw: 5'- gagatcagatctatcccagggttcagccag -3' Rv: 5'- gagatcgaattcttagctgtgatgtaccaggc -3'	BgIII EcoRI	(Lck-)mCherry-PLEKHG2-DH
Fw: 5'- gagatcagatctatcccagggttcagccag -3' Rv: 5'- gagatcgaattcttagttctcaagaagagggcgc -3'	BgIII EcoRI	(Lck-)mCherry-PLEKHG2-DHPH
Fw: 5'- gagatcaagcttttagctctgaccccaggag -3' Rv: 5'- gagatcggatccttagctgttccggtccg -3'	HindIII BamHI	(Lck-)mCherry-PLEKHG4-DH
Fw: 5'- gagatcaagcttttagctctgaccccaggag -3' Rv: 5'- gagatcggatccttagctctcaaaagcagg -3'	HindIII BamHI	(Lck-)mCherry-PLEKHG4-DHPH
Fw: 5'- gagatcctcagcggcctcctcaacgagatcttgg -3' Rv: 5'- gagatcggtagcttactcattgatgttgagcaaac -3'	XhoI Acc65I	(Lck-)mCherry-PREX1-DH
Fw: 5'- gagatcctcagcggcctcctcaacgagatcttgg -3' Rv: 5'- gagatcggtagctttagcgtctcccg -3'	XhoI Acc65I	(Lck-)mCherry-PREX1-DHPH

formaldehyde. After fixation, HUVECs were permeabilized for 5 min in PBS containing 0.5% Triton X-100 and blocked for 20 min in PBS containing 0.5% Bovine serum albumin (BSA). Finally, HUVECs were incubated for 1 h with directly labelled antibodies, dissolved in 0.5% PBS-BSA. Confocal images were obtained on a Nikon A1 confocal microscope, equipped with a 60x oil-immersion objective (NA 1.40, Plan Apochromat VC) and Nikon NIS elements software.

Live HUVEC FRET measurements

Glass coverslips with transfected HUVECs were mounted in Metal Atof fluor cell chambers at least 16 h after transfection. Live-cell FRET acquisitions were performed on a widefield Zeiss Axiovert 200 M microscope, equipped with an 40x oil-immersion objective (NA 1.30), Metamorph 6.1 software, a xenon arc lamp with monochromator (Cairn Research, Faversham, Kent, UK) and a cooled charged-coupled device camera (Coolsnap HQ, Roper Scientific, Tucson, AZ, USA). Cells were excited by using 420 nm light (slit width 30 nm) and a 455 DCLP (dichroic long-pass) mirror. Via a rotating filter wheel, CFP emission was directed to a 470/30 nm emission filter and YFP emission to a 535/30 nm emission filter. mCherry was excited with 570 nm light (slit width 10), and via a 585 DCXR mirror mCherry emission was directed to a 620/60 emission filter.

Data analysis

All image acquisitions were background corrected and YFP acquisitions were bleed-through corrected (55% leakage of the CFP into the YFP channel). FRET images in Figure 3 were obtained by ImageJ, according to refs [25,40].

YFP/CFP ratio analysis was performed in Matlab (Matlab, The MathWorks, Inc., Natick, Massachusetts, United States). The Matlab script was first described in ref [36]. Theil–Sen estimation analysis was performed according to Supplemental Figure S1. Of note, median slopes were determined and shown in the graphs, since median values are less prone to outliers. The graphs were made with PlotsOfData [41], showing the data as jittered dots, the median YFP/CFP values as a line and the median ‘activity’ values as a circle with 95% confidence interval indicated by a bar. The 95% confidence interval for the median was obtained by bootstrapping (1000 samples).

Data availability

The data generated during this study is available at Zenodo.org: <https://zenodo.org/record/2548920>

Acknowledgments

We thank D. Webb (Vanderbilt University), H.C. Welch (Babraham Institute), J. van Buul (Sanquin Research), J.L. Zugaza (University of the Basque Country), M. Hayakawa (Tokyo University of Pharmacy and Life Sciences), W.J. Pannekoek (University Medical centre Utrecht), I.G. Macara (Vanderbilt University), K. Mizuno (Tohoku University), H. Ueda (Gifu university), D. Manor Case Western Reserve University, and L.J. Bruurs (University Medical centre Utrecht) for providing us with the FL GEF constructs.

Disclosure statement

No potential conflict of interest was reported by the authors.

ORCID

Joachim Goedhart  <http://orcid.org/0000-0002-0630-3825>

References

- [1] Ridley AJ. Rho GTPases and actin dynamics in membrane protrusions and vesicle trafficking. *Trends Cell Biol.* 2006;16:522–529.
- [2] Madaule P, Axel R. A novel ras-related gene family. *Cell.* 1985;41:31–40.
- [3] Etienne-Manneville S, Hall A. Rho GTPases in cell biology. *Nature.* 2002;420:629–635.
- [4] Cherfils J, Zeghouf M. Regulation of small GTPases by GEFs, GAPs, and GDIs. *Physiol Rev.* 2013;93:269–309.
- [5] Fort P, Blangy A. The evolutionary landscape of Dbl-Like RhoGEF families: adapting eukaryotic cells to environmental signals. *Genome Biol Evol.* 2017;9:1471–1486.
- [6] Zheng Y. Dbl family guanine nucleotide exchange factors. *Trends Biochem Sci.* 2001;26:724–732.
- [7] Aittaleb M, Boguth CA, Tesmer JJG. Structure and function of heterotrimeric G protein-regulated Rho guanine nucleotide exchange factors. *Mol Pharmacol.* 2010;77:111–125.
- [8] Rossman KL, Sondek J. Larger than Dbl: new structural insights into RhoA activation. *Trends Biochem Sci.* 2005;30:163–165.
- [9] Erickson JW, Cerione RA. Structural elements, mechanism, and evolutionary convergence of Rho protein-guanine nucleotide exchange factor complexes. *Biochemistry.* 2004;43:837–842.
- [10] Rossman KL, Der CJ, Sondek J. GEF means go: turning on RHO GTPases with guanine nucleotide-exchange factors. *Nat Rev Mol Cell Biol.* 2005;6:167–180.
- [11] Schmidt A, Hall A. Guanine nucleotide exchange factors for Rho GTPases: turning on the switch. *Genes Dev.* 2002;16:1587–1609.
- [12] Rittinger K. Snapshots form a big picture of guanine nucleotide exchange. *Sci Signal.* 2009;2:pe63.
- [13] Jaiswal M, Dvorsky R, Ahmadian MR. Deciphering the molecular and functional basis of Dbl family proteins: a novel systematic approach toward classification of

- selective activation of the Rho family proteins. *J Biol Chem.* 2013;288:4486–4500.
- [14] Viaud J, Gaits-Iacovoni F, Payrastra B. Regulation of the DH–PH tandem of guanine nucleotide exchange factor for Rho GTPases by phosphoinositides. *Adv Biol Regul.* 2012;52:303–314.
- [15] Bryan BA, D’Amore PA. What tangled webs they weave: Rho-GTPase control of angiogenesis. *Cell Mol Life Sci.* 2007;64:2053–2065.
- [16] Beckers CML, van Hinsbergh VWM, van Nieuw Amerongen GP. Driving Rho GTPase activity in endothelial cells regulates barrier integrity. *Thromb Haemost.* 2009;103:40–55.
- [17] Broman MT, Mehta D, Malik AB. Cdc42 regulates the restoration of endothelial adherens junctions and permeability. *Trends Cardiovasc Med.* 2007;17:151–156.
- [18] Amado-Azevedo J, Reinhard NR, van Bezu J, et al. A CDC42-centered signaling unit is a dominant positive regulator of endothelial integrity. *Sci Rep.* 2017;7:10132.
- [19] Van Buul JD, Geerts D, Rho HS. GAPs and GEFs: controlling switches in endothelial cell adhesion. *Cell Adhes Migr.* 2014;8:108–124.
- [20] Hernández-García R, Iruela-Arispe ML, Reyes-Cruz G, et al. A systematic analysis of their expression profiles in VEGF-stimulated and tumor endothelial cells. *Vascul Pharmacol.* 2015;74:60–72.
- [21] Amado-Azevedo J, de Menezes RX, van Nieuw Amerongen GP, et al. A functional siRNA screen identifies RhoGTPase-associated genes involved in thrombin-induced endothelial permeability. *PLoS One.* 2018;13:e0201231.
- [22] Schultz J, Milpetz F, Bork P, et al. SMART, a simple modular architecture research tool: identification of signaling domains. *Proc Natl Acad Sci U S A.* 1998;95:5857–5864.
- [23] Van Rijssel J, Timmerman I, Van Alphen FPJ, et al. The Rho-GEF trio regulates a novel pro-inflammatory pathway through the transcription factor Ets2. *Biol Open.* 2013;2:569–579.
- [24] van Rijssel J, Kroon J, Hoogenboezem M, et al. The Rho-guanine nucleotide exchange factor trio controls leukocyte transendothelial migration by promoting docking structure formation. *Mol Biol Cell.* 2012;23:2831–2844.
- [25] Timmerman I, Heemskerk N, Kroon J, et al. A local VE-cadherin and Trio-based signaling complex stabilizes endothelial junctions through Rac1. *J Cell Sci.* 2015;128:3041–3054.
- [26] Kedziora KM, Leyton-Puig D, Argenzio E, et al. Rapid remodeling of invadosomes by Gi-coupled receptors. *J Biol Chem.* 2016;291:4323–4333.
- [27] Fritz RD, Pertz O. The dynamics of spatio-temporal Rho GTPase signaling: formation of signaling patterns. *F1000Res.* 2016;5:749.
- [28] Pasteris NG, Buckler J, Cadle AB, et al. Genomic organization of the faciogenital dysplasia (FGD1; Aarskog Syndrome) gene. *Genomics.* 1997;43:390–394.
- [29] Pasteris NG, Cadle A, Logie LJ, et al. Isolation and characterization of the faciogenital dysplasia (Aarskog-Scott syndrome) gene: a putative Rho/Rac guanine nucleotide exchange factor. *Cell.* 1994;79:669–678.
- [30] Welch HCE. Regulation and function of P-Rex family Rac-GEFs. *Small GTPases.* 2015;6:49–70.
- [31] Pannekoek W-J, Vliem MJ, Bos JL. Multiple Rap1 effectors control Epa1-mediated tightening of endothelial junctions. *Small GTPases.* 2018;1–8. DOI:10.1080/21541248.2018.1431512
- [32] Hernández-Vásquez MN, Adame-García SR, Hamoud N, et al. Cell adhesion controlled by adhesion G protein-coupled receptor GPR124/ADGRA2 is mediated by a protein complex comprising intersectins and Elmo-Dock. *J Biol Chem.* 2017;292:12178–12191.
- [33] Ando K, Fukuhara S, Moriya T, et al. Rap1 potentiates endothelial cell junctions by spatially controlling myosin II activity and actin organization. *J Cell Biol.* 2013;202:901–916.
- [34] Xu Z, Gakhar L, Bain FE, et al. The Tiam1 guanine nucleotide exchange factor is auto-inhibited by its pleckstrin homology coiled-coil extension domain. *J Biol Chem.* 2017;292:17777–17793.
- [35] López-Lago M, Lee H, Cruz C, et al. Tyrosine phosphorylation mediates both activation and downmodulation of the biological activity of Vav. *Mol Cell Biol.* 2000;20:1678–1691.
- [36] van Unen J, Reinhard NR, Yin T, et al. Plasma membrane restricted RhoGEF activity is sufficient for RhoA-mediated actin polymerization. *Sci Rep.* 2015;5:14693.
- [37] Inoue T, Do HW, Grimley JS, et al. An inducible translocation strategy to rapidly activate and inhibit small GTPase signaling pathways. *Nat Methods.* 2005;2:415–418.
- [38] Guntas G, Hallett RA, Zimmerman SP, et al. Engineering an improved light-induced dimer (iLID) for controlling the localization and activity of signaling proteins. *Proc Natl Acad Sci U S A.* 2015;112:112–117.
- [39] Reinhard NR, Mastop M, Yin T, et al. The balance between Gai-Cdc42/Rac and Ga12/13-RhoA pathways determines endothelial barrier regulation by sphingosine-1-phosphate. *Mol Biol Cell.* 2017;28:3371–3382.
- [40] Reinhard NR, van Helden SF, Anthony EC, et al. Spatiotemporal analysis of RhoA/B/C activation in primary human endothelial cells. *Sci Rep.* 2016;6:25502.
- [41] Postma M, Goedhart J. PlotsOfData—A web app for visualizing data together with their summaries. *PLOS Biol.* 2019;17:e3000202.